Spectral Properties of Induced and Evoked Gamma Oscillations in Human Early Visual Cortex to Moving and Stationary Stimuli

J. B. Swettenham, S. D. Muthukumaraswamy, and K. D. Singh
Cardiff University Brain Research Imaging Centre, School of Psychology, Cardiff University, Cardiff, United Kingdom

Swettenham JB, Muthukumaraswamy SD, Singh KD. Spectral properties of induced and evoked gamma oscillations in human early visual cortex to moving and stationary stimuli. *J Neurophysiol* 102: 1241–1253, 2009. First published June 10, 2009; doi:10.1152/jn.91044.2008. In two experiments, magnetoencephalography (MEG) was used to investigate the effects of motion on gamma oscillations in human early visual cortex. When presented centrally, but not peripherally, stationary and moving gratings elicited several evoked and induced response components in early visual cortex. Time-frequency analysis revealed two nonphase locked gamma power increases—an initial, rapidly adapting response and one sustained throughout stimulus presentation and varying in frequency across observers from 28 to 64 Hz. Stimulus motion raised the sustained gamma oscillation frequency by a mean of ~10 Hz. The largest motion-induced frequency increases were in those observers with the lowest gamma response frequencies for stationary stimuli, suggesting a possible saturation mechanism. Moderate gamma amplitude increases to moving versus stationary stimuli were also observed but were not correlated with the magnitude of the frequency increase. At the same site in visual cortex, sustained alpha/beta power reductions and an onset evoked response were observed, but these effects did not change significantly with the presence of motion and did not correlate with the magnitude of gamma power changes. These findings suggest that early visual areas encode moving and stationary percepts via activity at higher and lower gamma frequencies, respectively.

INTRODUCTION

The presence and modulation of neuronal oscillations within specific frequency bands appear to be fundamental to the implementation of perception and cognition within the brain (Engel et al. 1992, 2001; Palva and Palva 2007) although this has not been without controversy (Pareti and De Palma 2004). Oscillations can be generated in long-range networks that may reflect inter-regional binding and information transfer or can occur in local cortical networks that are task-specific and reflect the functional modularity of the brain. One such oscillation is the gamma oscillation, loosely defined as ~20–100 Hz. As well as being selective for specific visual stimuli, gamma oscillations have been proposed as a temporal coding scheme through which distributed neuronal groups are able to become synchronous—allowing communication between these areas and underlying the "binding" of stimulus features (Fries et al. 2007; Gray et al. 1989; Womelsdorf and Fries 2006). Other studies have implicated gamma frequency oscillations in processes such as attention and memory (Jensen et al. 2007) and visual perception (Melloni et al. 2007), including the

perception of visual illusions (Parra et al. 2005), object perception (Tallon-Baudry and Bertrand 1999), and hallucinations (Behrendt and Young 2004).

Within primary visual area V1, stimulus-related gamma oscillations have been observed and characterized in both cat (Eckhorn et al. 1988;) Gray et al. 1989, 1990; Kayser et al. 2003; Kruse and Eckhorn 1996; Siegel and König 2003) and macaque (Belitski et al. 2008; Friedman-Hill et al. 2000; Frien et al. 2000; Gail et al. 2004; Henrie and Shapley 2005; Maldonado et al. 2000; Rols et al. 2001; Shapley et al. 2003) under both anesthetized and awake states. A common finding of these studies is that nonphase-locked, i.e., induced rather than evoked, gamma oscillations are elicited by visual stimulation and are modulated by stimulus properties more than oscillations at other frequencies. For example, the amplitude of gamma oscillations increases with stimulus contrast (Henrie and Shapley 2005) and is modulated by orientation (Friedman-Hill et al. 2000; Frien et al. 2000; Siegel and König 2003). In addition, and of particular interest to our study, in the awake macaque the mean frequency of gamma oscillations is higher for drifting compared with stationary gratings (Friedman-Hill et al. 2000).

It is not immediately clear whether methods such as electroencephalography (EEG) or MEG, which measure activity from very large numbers of neurons, would reveal the richness and specificity of responses observed intracortically with measures such as local field potentials (LFPs)—which are thought to originate within just 500 μm of the electrode tip (Henrie and Shapley 2005; Kruse and Eckhorn 1996). However, several studies indicate that robust gamma effects can be measured extracortically (Adjamian et al. 2004; Hall et al. 2005; Hoogenboom et al. 2006; Rols et al. 2001). Using surface electrocortigrams—which potentially bridge the gap between multiunit activity (MUA)/LFP recordings and scalp measures using EEG or MEG—Rols et al. (2001) demonstrated sustained, induced V1 gamma (40–55 Hz) oscillations and transient evoked responses to small luminance patch stimuli in two anesthetized macaques. In addition, a recent human MEG study showed 50 Hz gamma oscillations in primary visual cortex were modulated by spatial frequency, being tuned to an optimal spatial frequency of ~3 cycles per degree (cpd) (Adjamian et al. 2004). This is consistent with the spatial tuning properties of macaque V1 cells (Foster et al. 1985), and the optimum spatial frequency for contrast detection in human (Campbell and Robson 1968). Also using MEG, Hall et al. (2005) demonstrated that gamma oscillations in human primary visual cortex increased monotonically with stimulus contrast. In macaque, a similar relationship had been reported between contrast and the magnitude of the functional magnetic resonance imaging

Address for reprint requests and other correspondence: K. D. Singh, Cardiff University Brain Research Imaging Centre (CUBRIC), School of Psychology, Cardiff University, Park Place, Cardiff CF10 3AT, UK (E-mail: singhkd @cardiff.ac.uk).

(fMRI) blood-oxygen-level-dependent (BOLD) response as well as gamma oscillations in the LFP and MUA (Logothetis et al. 2001). However, there are instances when the BOLD response and gamma oscillations do not correlate. For example, in a direct MEG/fMRI comparison experiment, using the same grating stimuli, when spatial frequency increased from 0.5 to 3.0 cpd, there was a 300% increase in the power of gamma oscillations in primary visual cortex, whereas the BOLD response did not change in amplitude (Muthukumaraswamy and Singh 2008).

The general aim of the current study is to investigate the effect of another stimulus domain, motion, on the spectral properties of oscillatory responses in human early visual cortex and to relate these findings to previous animal neurophysiological results and human neuroimaging. In anesthetized cat, the frequency of gamma oscillations increased with stimulus velocity, but responses were negligible to static stimuli (Gray et al. 1990). However, in awake macaque, moving and static stimuli generated gamma oscillations of the same amplitude, although again at higher frequencies for moving compared with static stimuli (Friedman-Hill et al. 2000). In contrast, human EEG studies have shown that posterior gamma oscillation magnitude is significantly greater for moving than static dot stimuli and greater for coherent than incoherent motion (Krishnan et al. 2005). No differential effects on gamma frequency were reported. Finally, in human fMRI, motion increases the BOLD response in V1 by between 30 and 50% (Singh et al. 2000; Tootell et al. 1995). Thus there are some conflicting indications of how stimulus motion might modulate the spectral properties of evoked and induced responses measured from human early visual cortex with MEG. If gamma oscillations, measured and localized using MEG, reflect the underlying properties of MUA/LFP neuronal ensembles, our hypothesis is that motion will increase the frequency of gamma oscillations in early visual cortex. Similarly, if gamma oscillation amplitudes are tightly coupled to the BOLD response, previous fMRI studies suggest that the presence of stimulus motion should increase gamma amplitude.

METHODS

A total of 15 observers (9 male and 6 female, aged 19–41 yr) consented to participate in the study, which adhered to the tenets of the Declaration of Helsinki and was approved by the School of Psychology Ethics Committee, Cardiff University. Five observers took part in both experiments. Observers had normal or corrected-to-normal vision and no history of neurological dysfunction or injury. All observers had previously acquired anatomical magnetic resonance (MR) scans.

Experiment 1

In the first study, stimuli were high contrast, achromatic, horizontal, 3 cpd square-wave gratings (6 × 6°) that were either stationary or drifting at 1.33°/s (4 Hz). The spatial frequency and contrast were chosen to be optimal for generating gamma oscillations in human primary visual cortex as measured with MEG (Adjamian et al. 2004), and the velocity was within the range known to generate strong BOLD responses (Singh et al. 2000). The stimuli were viewed binocularly in the lower right visual field with the top left corner of the grating at fixation (indicated by a continuously present red circle). Throughout the experiment, the background was gray and isoluminant with the gratings, which had close to 100% luminance contrast. There were

100 trials—each trial was 8 s duration and had four phases of 2 s each. These phases were always presented in the following order: blank screen, stationary grating, drifting grating, and blank screen. In addition there were 10 catch trials in which the drifting phase was replaced with a blank phase. For each trial, the direction of the grating drift was pseudo-randomly selected to be upward or downward. Ten observers (5 males, 5 females; 19–41 yr) participated in the study and they were instructed to maintain fixation and press a button when the grating disappeared (i.e., after the stationary phase in the catch trials else after the moving phase).

Experiment 2

In a second study, the stationary and drifting gratings were presented in separate randomized trials to rule out expectation or other order effects. The effect of foveal versus peripheral stimulation was also studied. The top left corner of the grating was either at fixation (as in previous experiment) or 4° to the right and 4° below fixation (total distance 5.7°); gratings were 4 × 4°; and the moving gratings always drifted upward. There were 50 trials of each condition (still, 0.0°; still, 5.7°.; moving, 0.0°.; moving, 5.7°) presented in pseudorandom order. The duration of each grating presentation was jittered between 2.0 and 2.4 s and was preceded by 3.1 s of blank screen. Observers were instructed to maintain fixation and press a button when the grating disappeared. Ten observers (7 males, 3 females; 25–41 yr) participated in the study.

Recording and analysis

Stimuli were presented on a Mitsubishi Diamond Pro 2070 monitor and were controlled by a ViSaGe visual stimulus generator (Cambridge Research Systems, Kent, UK). The screen size was 1,024 × 768 pixels, and the monitor frame rate was 100 Hz. The monitor was outside the magnetically shielded room and viewed directly from within, at 2.15 m, through a cut-away portal in the shield. Separate to the MEG recordings, a photodiode on the monitor screen was used to measure the spectral properties of the presented stimulus. This confirmed that when the grating moved, there was a clear resolved peak at 4 Hz (the equivalent temporal frequency) and that no extra power was observed in the gamma frequency range. In addition, an MEG recording performed without a participant confirmed that, within the occipital MEG sensors, no noise within the gamma frequency range was induced by the stimulus. The only observable contamination was at the frame-rate of the monitor i.e., at 100 Hz.

MEG data were recorded in a dimly lit, magnetically shielded room using a 275-channel whole-head radial gradiometer system (VSM MedTech) in a single unaveraged run at a sampling rate of 1,200 Hz. An additional 29 reference channels were recorded for noise-cancellation purposes, and the primary sensors were analyzed as synthetic third-order gradiometers (Vrba and Robinson 2001). Three of the 275 channels were turned off due to excessive sensor noise. Data collection took ~15 (*experiment 1*) and 18 (*experiment 2*) minutes. Eye movements were not recorded during the scanning sessions. The observer was fitted with three electromagnetic head coils that were localized relative to the MEG system immediately before and after the recording session. The mean head movement was 0.49 ± 0.29 (SD) cm. Outside the shielded room, a three-dimensional digitizer (Fastrak; Polhemus) was used to determine the position of these coils relative to the surface of the observer's head. This head surface was matched to the observer's own MR-defined head shape, and these fiduciary locations could be verified using high-resolution digital photographs.

Off-line, each data set was band-pass-filtered using a fourth-order bidirectional IIR Butterworth filter into 10 Hz width frequency bands between 10 and 100 Hz. For comparison of low with high gamma frequencies, 30 to 60 and 60 to 90 Hz bands were also used. Evenly spaced frequency bands were used so that the accuracy of covariance

matrix estimation would be equal for each frequency band (Brookes et al. 2008). The synthetic aperture magnetometry (SAM) beamformer algorithm as implemented in the CTF software (Robinson and Vrba 1999) was used to create differential images of source power (pseudo-T statistics) for 2 s of baseline (-2 to 0 s) compared with 2 s of visual stimulation (0–2 s). Time windows for baseline estimation were of equal duration to the time window of interest to achieve balanced covariance estimation. Details of the calculation of SAM pseudo-T source image statistics are described in detail in a number of sources ((Cheyne et al. 2003; Hillebrand and Barnes 2005; Hillebrand et al. 2005; Singh et al. 2003; Vrba and Robinson 2001). For source localization, a multiple, local-spheres-forward model was derived by fitting spheres to the brain surface extracted by BET (Huang et al. 1999). Estimates of the three-dimensional distribution of source power were derived for each observer's whole head at 3-mm isotropic voxel resolution. Note that eye blinks were not removed from the data because, in the unlikely event that blinks were time locked to the stimuli, the SAM spatial filter will localize blink-related artifacts to the eyes (Bardouille et al. 2006). As these eye activations can indicate the possibility of associated, transient, induced gamma activity in occipital cortex (Bardouille et al. 2006), the SAM reconstructions were inspected for evidence of this artifact.

For group analysis, images were normalized into Montreal Neurological Institute (MNI) template space using an automated linear (affine) registration tool—FLIRT (www.fmrib.ox.ac.uk/analysis/research/flirt). Nonparametric permutation tests were conducted using the full permutation set (1,024) for each condition with 5 mm spatial smoothing of the interparticipant variance and thresholded using the omnibus test statistic value (obtained from the distribution of the largest activations in the whole volume, not each voxel, and so dealing with the multiple comparison problem) at $P < 0.05$ (Nichols and Holmes 2002; Singh et al. 2003).

Individual and group SAM images were visualized using mri3dX (https://cubric.psych.cf.ac.uk/Documentation/mri3dX/) and freesurfer (https://surfer.nmr.mgh.harvard.edu/fswiki).

For spatial locations of interest, activation time courses were calculated as if a sensor or an electrode were at that position, i.e., a virtual electrode. Time courses were constructed using SAM beamformer coefficients obtained using the individual condition covariance matrices band-pass filtered between 0 and 100 Hz (Robinson and Vrba 1999). For each of these virtual-electrode time courses, time-frequency spectrograms were generated by determination of the time-varying amplitudes at each sample frequency. These envelopes were formed from the amplitude of the analytic signal derived using the Hilbert Transform. The resulting spectrograms were either calculated separately for each trial and then averaged, to reveal both induced and evoked responses, or the spectrogram of the average across all trials was calculated to reveal the time-frequency content of the evoked responses. Here we present spectrograms as a percentage change from the mean baseline power at each frequency. SPSS 12.0 was used to perform paired t-test and Pearson's correlations between the moving and stationary conditions for frequency and amplitude values at these locations.

RESULTS

Experiment 1

SAM analyses were performed for nine nonoverlapping frequency bands of 10 Hz width between 10 and 100 Hz and over 2-s time windows (pre- vs. post- stationary grating onset). Viewing stationary gratings in the right visual field primarily elicited an increase in gamma frequency (>30 Hz) power in early visual areas of the left hemisphere. To illustrate this, Fig. 1A shows the left hemisphere of each observer's co-registered, anatomical MR scan viewed from the midline and with the cortical surface partially inflated. Superimposed are the SAM-derived statistical estimates in the frequency band that contained the largest power changes in the occipital lobe. For 8 of 10 observers (*observers A–H*), this was the largest power change in the brain, whereas for *observers I* and *J,* the largest power change occurred in the frontal lobe (at 80–90 and 70–80 Hz, respectively), and the second largest power change was at 30–40 Hz in visual cortex. Power changes were not observed in the eyes, indicating that eye blinks were not time locked to stimulus presentation (Bardouille et al. 2006). *Observer J* did not show a response in medial visual cortex so is omitted from Fig. 1A. In the other nine observers, gamma power increases were observed in (or close to) the calcarine sulcus suggesting a primary visual cortex location as the source of these gamma oscillations. Note that there is substantial inter-observer variability in the frequency of these gamma oscillations.

The group effects of viewing stationary gratings were investigated using permutation analysis of the spatially normalized SAM data (Singh et al. 2003). Consistent with the individual observer data, there were areas of significantly increased gamma frequency power in the early visual areas of the left hemisphere. Figure 1B shows images from the permutation analyses for each of the 10 Hz frequency bands over 2 s time windows. The orange-yellow color overlay indicates voxels with significantly ($P < 0.05$, 2-tailed) increased power and these are shown on the left hemisphere of the MNI template brain, viewed from the midline and with the cortical surface partially inflated. The largest mean power change occurred in the 50 to 60 Hz frequency band.

Time-frequency plots were generated for each observer at the location of their largest occipital power change in response to stationary gratings. Figure 1, *C* and *D,* shows plots for three observers and mean time-frequency plots for the group ($n = 10$). Inspection of the evoked neural response (Fig. 1D) revealed a broadband, transient increase in energy associated with changes in the stimulus (i.e., at 0, 2, and 4 s). An analysis of both induced and evoked effects (Fig. 1C) revealed further features including: both stationary (0–2 s) and moving (2–4 s) gratings elicited an increase in gamma frequency power that was sustained throughout presentation; the sustained increase in power associated with moving gratings was centered at a higher frequency than that associated with stationary gratings (see following text); the presentation of gratings produced a reduction in power in alpha and beta bands (<25 Hz) that appears more pronounced during the moving phase (see following text); and ~750 ms after the offset of the moving gratings, there was a rebound increase in alpha and beta band energies.

The frequency at which the largest percentage change from baseline occurred, and the amplitude of this change for the period 1–2 s after onset of the stationary and moving gratings, were obtained for each observer. There was considerable inter-observer variation in the peak gamma frequencies [stationary: 27.0–55.5 Hz, 43.5 ± (SD) 9.0 Hz; moving: 40.0–66.0 Hz, 51.0 ± 7.7 Hz]. Despite this large variability, paired t-test confirmed that moving gratings were associated with significantly higher gamma frequencies ($P = 0.01$) and higher-amplitude power increases (stationary: 26.2 ± 17.3%; moving: 34.4 ± 18.2%; $P = 0.04$). Similar analysis for the alpha frequency band, 0.5–2 s after onset of the stationary and
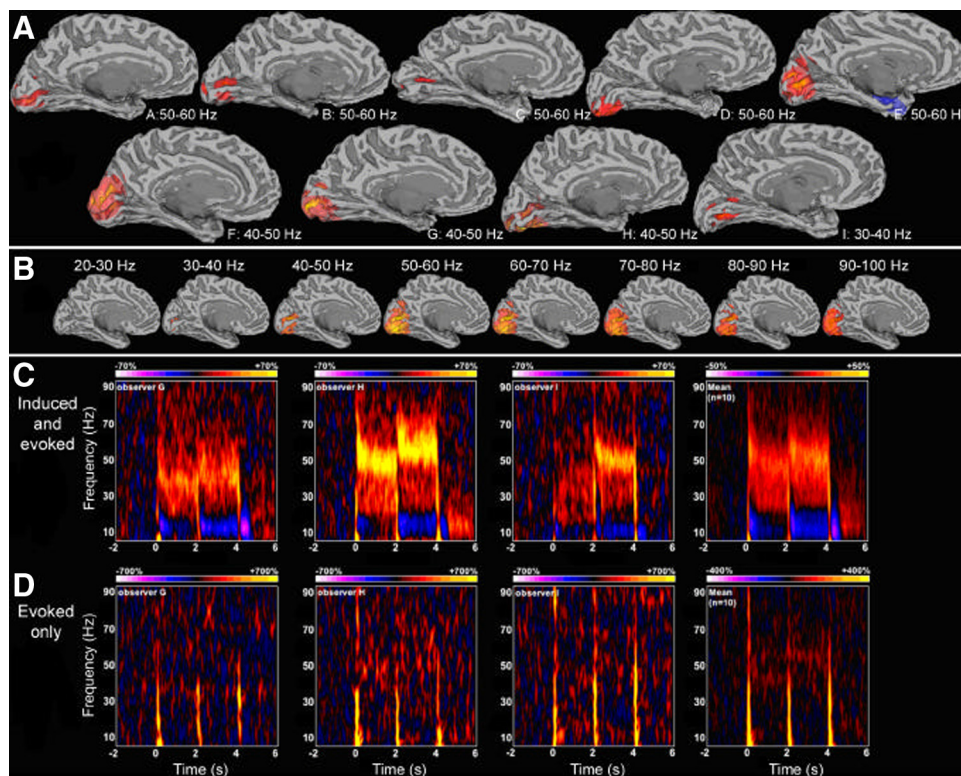
FIG. 1. Spatial localization and time-frequency characteristics of stimulus driven responses in *experiment 1*. In all images, the colors represent power changes from baseline with orange/red/yellow depicting power increases and blue/purple/pink power decreases. *A*: individual synthetic aperture magnetometry (SAM) images for each of 9/10 observers, showing statistical estimates of power changes within the frequency band (between 10 and 100 Hz) that gave the largest response in the occipital lobe to stationary gratings (−2–0 vs. 0–2 s). The left hemisphere is viewed from the midline with the cortex inflated by 50%. *Observer J* did not demonstrate medial occipital gamma and is not shown. In the cortex, dark and light gray regions represent sulci and gyri, respectively. The color overlay indicates the amplitude of the pseudo-T statistic ($2 \leq t \leq 8$). *B*: group ($n = 10$) SAM images showing significant ($P < 0.05$ corrected) regions of increased power in response to stationary gratings (−2–0 vs. 0–2 s) superimposed on the left hemisphere of the Montreal Neurological Institute (MNI) template brain. Each panel shows the response for a 10-Hz width frequency band (between 20 and 100 Hz) as indicated. The largest mean power change was at 50–60 Hz in Brodmann area 17 ($t = 9.27$; MNI: −11.0 −89.3 −3.0). *C* and *D*: time-frequency plots are shown for each of 3 representative observers (and the mean observer, $n = 10$) from *experiment 1* at the location of the largest response in visual cortex. In all cases, this occurred at gamma frequencies and voxels were in early visual cortex of the left hemisphere. *C* shows the average of the time-frequency representations for each trial and hence reveals both evoked and induced activity. *D* shows the time-frequency representation of the average over all trials and hence depicts only evoked activity.

moving gratings, revealed no difference in the frequency of the largest proportional change from baseline ($P = 0.4$). However, the magnitude of the reduction in alpha frequency power was greater in the moving than the stationary condition ($P = 0.03$).

Experiment 2

In the previous experiment, the stationary grating always preceded the drifting grating to prevent motion aftereffects contaminating the response to stationary gratings. However, this leaves the possibility that the differences in neural activity observed in response to stationary versus moving gratings may have been influenced by the order of presentation. In addition, the time-frequency plots shown in Fig. 1 were computed for locations indicated by SAM analyses of neural activity during viewing of stationary gratings. It is therefore possible that these locations were not optimal to illustrate the neural response to moving gratings. To resolve this, the second experiment was performed with moving and stationary gratings presented in different trials. In addition, there were two different presentation positions of the grating stimulus—either in the central or peripheral visual field.

As with *experiment 1,* for 9 of 10 observers, the principal neural response to both stationary and moving gratings viewed centrally

was an increase in gamma frequency power in early visual areas of the left hemisphere (Fig. 2*A*). In contrast, peripherally viewed stationary and moving gratings did not elicit robust, statistically significant gamma increases in visual areas (Fig. 2*B*).

Time-frequency plots were generated for the nine observers who showed an occipital increase in gamma frequency power in response to centrally viewed gratings. For stationary and moving gratings, plots were calculated at the location of the largest occipital power change observed from SAM analyses in 10 Hz width frequency bands (between 10 and 100 Hz). In all cases, this was in the gamma band, and for seven of nine observers the frequency band was higher in the moving than in the stationary condition (and for the other two observers it was the same frequency band). Figure 2*C* shows time-frequency plots for three observers and mean time-frequency plots for the group ($n = 9$), which clearly show the same components as in *experiment 1,* i.e., an initial broadband, transient evoked response (0.0–0.2 s); an early increased gamma frequency "spike" (0.2–0.5 s); a sustained gamma frequency response (1.0–2.0 s); and a sustained decrease in alpha frequency power (0.5–2.0 s). There is also clear confirmation of the key finding in *experiment 1* that moving gratings elicit sustained gamma oscillations at a higher frequency than stationary gratings.
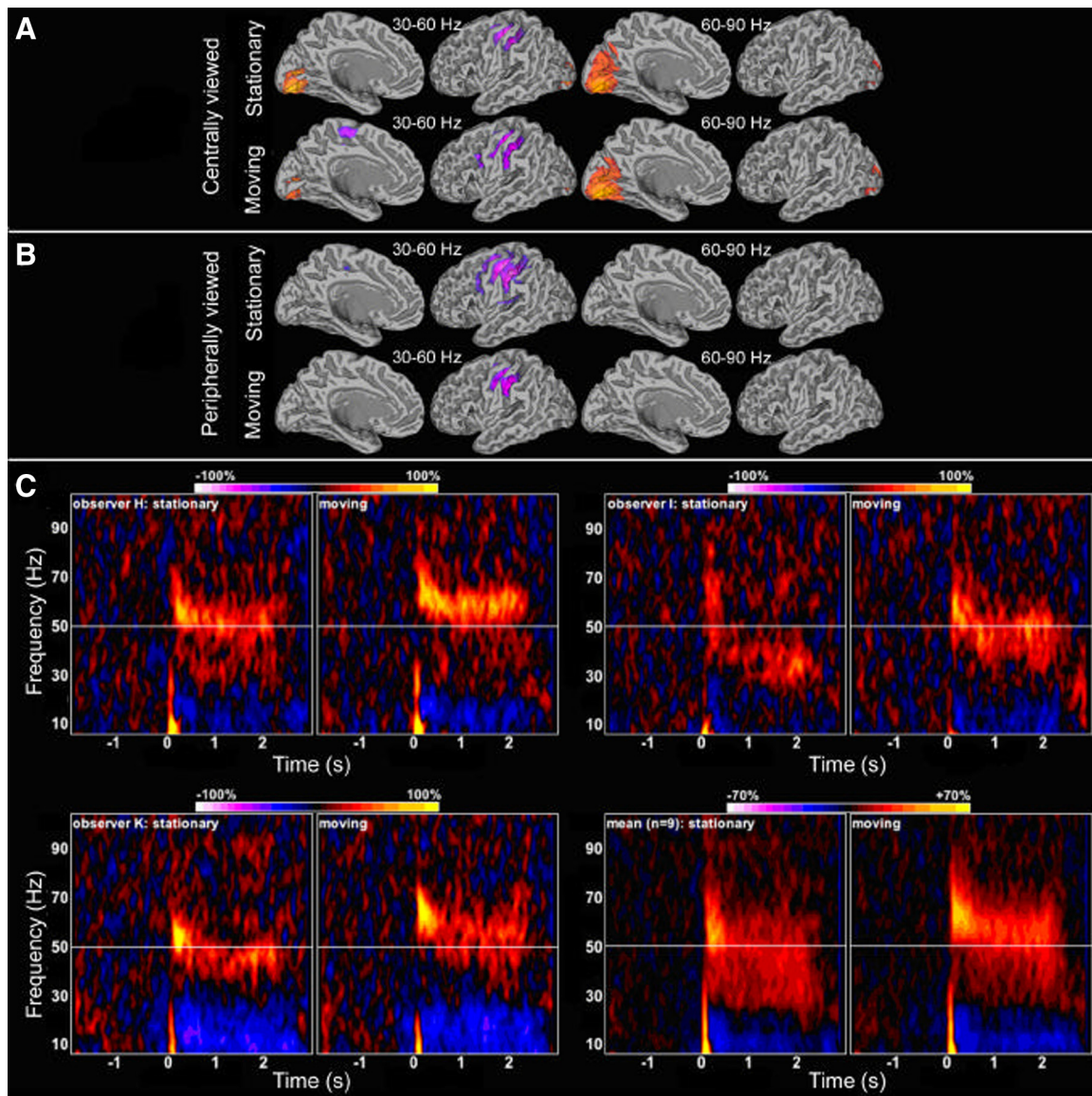
FIG. 2. Spatial localization and time-frequency characteristics of stimulus driven responses in *experiment 2*. In all images, the colors represent power changes from baseline with orange/red/yellow depicting power increases and blue/purple/pink power decreases. The location of statistically significant ($P < 0.05$, $n = 10$) group SAM power changes are shown for centrally viewed (*A*) and peripherally viewed (*B*) stationary and moving stimuli. The oscillatory power changes are shown overlaid on a 50% inflated model of the MNI template brain with dark and light gray regions representing sulci and gyri, respectively. In *C*, time-frequency plots are shown for each of 3 representative observers (and the mean observer, $n = 9$) from *experiment 2* at the location of the largest response in visual cortex. In all cases, this occurred at gamma frequencies and voxels were in early visual cortex of the left hemisphere. The plots show the average of the time-frequency representations for each trial and hence reveal both evoked and induced activity. The white line at 50 Hz has been added to better demonstrate the frequency shift between stationary and moving stimuli.

In Fig. 3, the temporal evolution of activity within these key frequency ranges are further investigated. At low frequencies (below 15 Hz, Fig. 3, *A* and *B*), the response is characterized by an evoked power increase at a latency of around 80–100 ms, followed by an induced decrease in power that begins at around 200 ms after stimulus onset and lasts for the entire presentation period. None of these effects are selective for the presence of motion. In the gamma range (Fig. 3, *D–F*), the initial evoked gamma onset "spike" is visible at around 130–250 ms. For lower gamma frequencies (45–55 Hz), this spike is larger for stationary stimuli, whereas for the higher ranges (55–85 Hz), the spike is greater for moving stimuli compared with stationary stimuli. Note that a stimulus evoked gamma response is visible up to around 85 Hz for moving stimuli (Fig. 3*F*), but no

significant gamma was observed at higher frequencies. If power is averaged across a wide range of frequencies (Fig. 3, *G* and *H*), then the evoked onset spike and sustained responses are both observed but show no differential effects for the presence of motion. This demonstrates the importance of a full time-frequency analysis to correctly identify stimulus-specific response behaviors. In general, the magnitude of the gamma response tended to fall over the first 1 s of stimulus presentation time but was stable for the latency range 1–2 s.

Figure 3*I* shows the conventional onset evoked response for stationary and moving stimuli and is generated by averaging the virtual-electrode time series for the peak location in early visual cortex across trials and observers. The responses show a standard VEP morphology with a large initial peak for both the
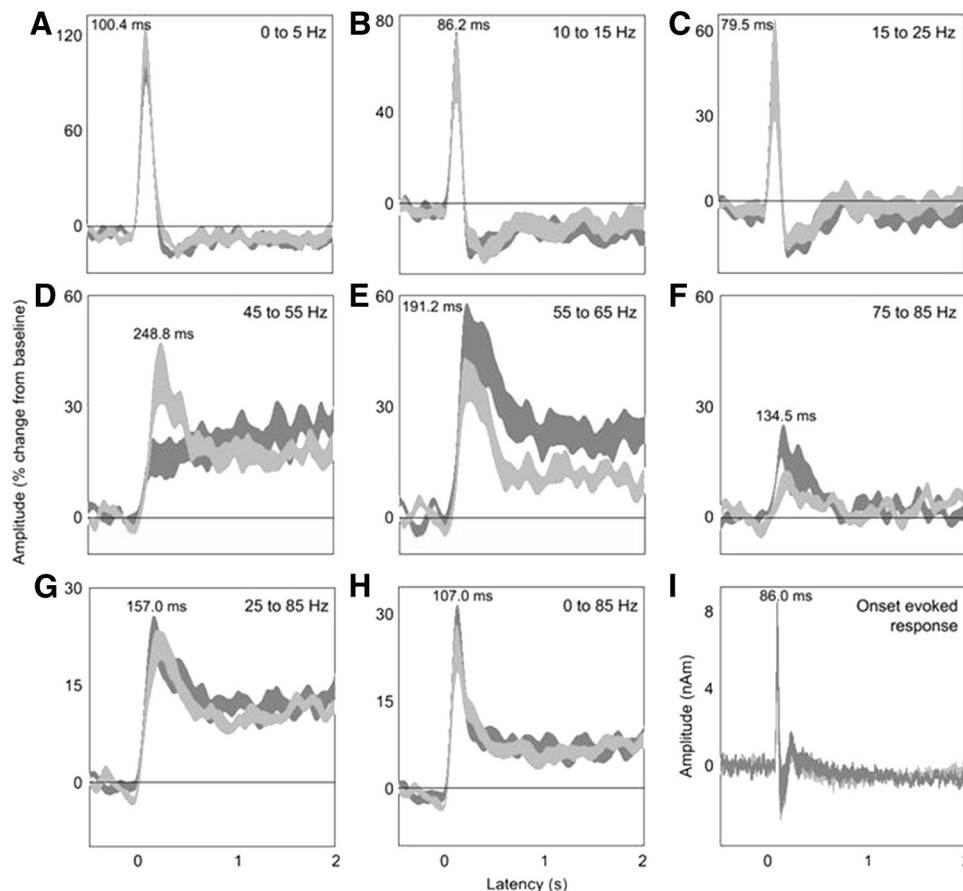
FIG. 3. Group average ($n = 9$) responses depicting the temporal evolution of the cortical response within primary visual cortex, for *experiment 2*. In all cases, the virtual-electrode response to stationary stimuli is shown in light-gray and the response to moving stimuli in dark gray. The shaded regions indicate the standard error on the mean across all participants. In *A–H*, the amplitude of response is plotted as a function of time for a range of frequency bands, chosen to illustrate the main effects found. In *I*, the onset evoked response is shown for the average virtual electrode in primary visual cortex. In contrast to the oscillatory responses depicted in *D–F*, no difference in onset evoked response amplitude or latency was found between stationary and moving stimuli.

moving (mean latency: 84 ± 18 ms; mean amplitude: 8 ± 4 nAm) and stationary (mean latency: 85 ± 14 ms; mean amplitude: 7 ± 3 nAm) conditions. Paired *t*-test confirmed there was no difference in either the latencies or the amplitudes of the peaks between the conditions ($P = 0.8$ and 0.2, respectively). The amplitude of the evoked responses in the moving and stationary conditions were very highly correlated across individuals ($r = 0.978$, $P < 0.001$). However, comparison of evoked response amplitudes in the moving and stationary conditions with the magnitude and frequency of the other neural components investigated, such as the induced gamma oscillations, showed low correlations ($r < 0.4$, $P > 0.3$ in all cases).

Figure 4 shows the shape and magnitude of the oscillatory power spectra, averaged over a set of key time periods, for the same virtual electrode positions. Again it can be seen that stimulus-evoked low-frequency power changes occur early after stimulus onset (Fig. 4*A*; 0–50 ms) but are not selective for the presence of motion. Alpha/beta power reductions are apparent from ~150 ms poststimulus onset and are sustained for the whole presentation period but are not modulated by the presence of motion (Fig. 4, *D–F*). At ~100 ms, gamma oscillations start to be visible in the power spectra for both stationary and moving stimuli (Fig. 4*C*). These peak in amplitude within the 200 to 250 ms time range (the evoked gamma spike; Fig. 4*E*) and show clearly a lower dominant frequency for stationary than moving stimuli. When power is averaged across the entire postspike presentation time (1–2 s; Fig. 4*F*), gamma oscillations are still present in the average spectra, albeit at a reduced amplitude and frequency. There is again an

obvious difference between the spectra for stationary and moving stimuli with moving stimuli demonstrating a higher sustained gamma frequency and a more peaked spectral profile.

For each observer, the frequency at which the largest proportional change from baseline occurred was noted and compared using paired *t*-test, between moving and stationary grating conditions. During the initial gamma "spike" (0.2–0.5 s), the moving condition showed the largest power changes at significantly higher mean frequencies than the stationary condition (stationary: 53.3 ± 8.2 Hz; moving: 61.4 ± 7.4 Hz; $P < 0.001$); however, there was no significant difference between the magnitude of the mean power changes (stationary: $49.2 \pm 20.3\%$; moving: $58.3 \pm 25.9\%$; $P = 0.1$). Similarly, during the sustained gamma component (1.0–2.0 s), the moving condition showed the largest power changes at significantly higher mean frequencies than the stationary condition (stationary: 43.8 ± 11.8 Hz; moving: 55.0 ± 4.5 Hz; $P = 0.006$). Again, there was no significant difference in the magnitude of the mean power changes (stationary: $27.7 \pm 6.3\%$; moving: $35.9 \pm 14.9\%$; $P = 0.08$).

Figure 5 shows in more detail the relationship between stationary and moving response magnitudes and frequencies for each observer. Moving stimuli always, except for a single data point, elicited a higher frequency oscillation than stationary stimuli, both for the initial gamma spike and the sustained induced gamma response. Although there appeared to be a similar trend for the gamma amplitudes (Fig. 5*B*), this was less compelling and, as stated in the preceding text, did not quite reach significance ($P = 0.08$).
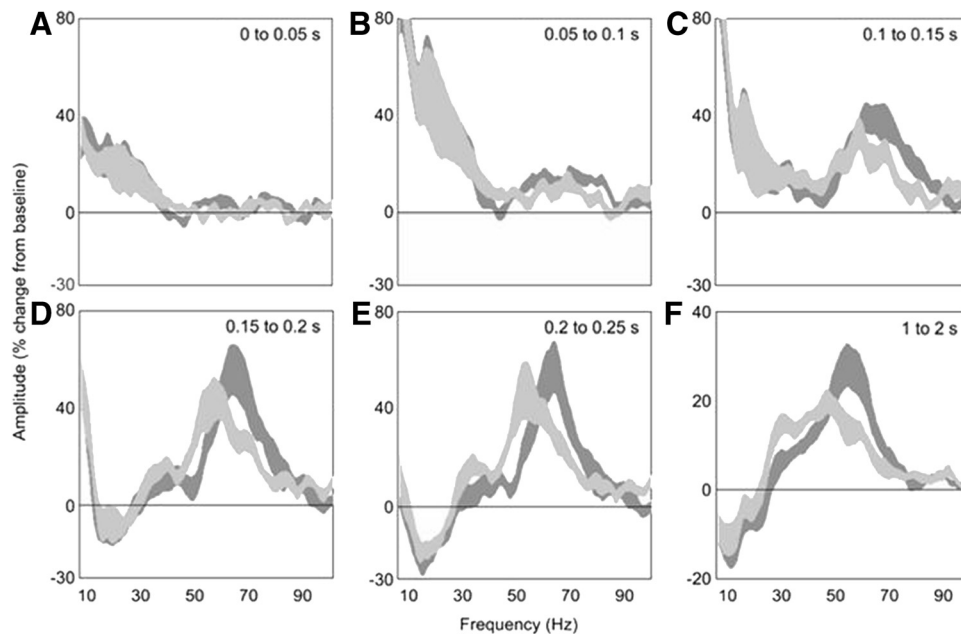
FIG. 4. Group average ($n = 9$) responses depicting the average power spectrum within primary visual cortex in *experiment 2*. In all cases, the virtual-electrode response to stationary stimuli is shown in light gray and the response to moving stimuli in dark gray. The shaded regions indicate the SE across all participants. These amplitude spectra, plotted as percentage changes from the prestimulus baseline, are shown for a variety of time-ranges, chosen to illustrate the main effects found. Low-frequency power increases are clearly evident in the early time ranges but are not selective for moving stimuli. Gamma responses start to occur at around 100 ms and are clearly different for moving stimuli, compared with stationary, at around 150–200 ms. For the later time ranges, the stimulus induced oscillatory change was greater for stationary gratings at ~30–50 Hz and for moving gratings at ~50–70 Hz. Note the apparent sharpening of the gamma spectrum for moving stimuli in the 1.0- to 2.0-s time period.

Further paired *t*-test showed that the frequency at which the largest power change occurred was higher for the early evoked gamma spike than the sustained gamma component for moving ($P = 0.006$) and stationary ($P = 0.004$) gratings. In addition, the magnitude of this power change was higher in the early gamma component than in the sustained gamma component for moving ($P = 0.001$) and stationary ($P = 0.003$) gratings. The magnitudes of the early and sustained gamma components for each individual were highly correlated with each other (moving: $r = 0.905$, $P = 0.001$; stationary: $r = 0.815$, $P = 0.007$). In addition, magnitudes of power changes between the moving and stationary conditions were highly correlated for the early component ($r = 0.812$, $P = 0.008$) while the sustained gamma was moderately correlated ($r = 0.623$, $P = 0.07$).

Finally, although the magnitudes of the reductions in alpha frequency power between the moving and stationary conditions were highly correlated ($r = 0.825$, $P = 0.006$), there was little correlation between alpha frequency power reduction and the magnitude of the early or sustained gamma response (early: moving, $r = 0.474$, $P = 0.2$; stationary, $r = 0.592$, $P = 0.07$; sustained: moving, $r = 0.303$, $P = 0.4$; stationary, $r = 0.546$, $P = 0.1$).

The gamma oscillations showed large inter-observer variability in both magnitude and frequency and are illustrated in Fig. 6. For the initial evoked gamma spike (Fig. 6*A*), the predominant effect of stimulus motion is a shift upward in frequency without much of a change in shape of the inter-observer variances, either in frequency or amplitude. For the sustained gamma response (Fig. 6*B*), the same shift upward in frequency can be seen, but there is also more variance evident in the amplitude of responses, and less variance in the peak oscillation frequency. The biggest increases in gamma frequency occurred in those observers with the lowest intrinsic gamma oscillation frequency for stationary stimuli (Fig. 6, *C* and *D*). In fact, the increase in frequency with motion, and the stationary frequency were highly negatively correlated across observers (Fig. 6*D*). This suggests a fundamental limit beyond which gamma oscillations are not observed. However, note that no significant correlation was found between gamma response amplitude and gamma response frequency in the two time periods studied for either the stationary or moving conditions.

Finally, we used the data from the static trials to investigate how a reduction in stimulus duration would affect the accuracy of the SAM source reconstructions, assuming our relatively
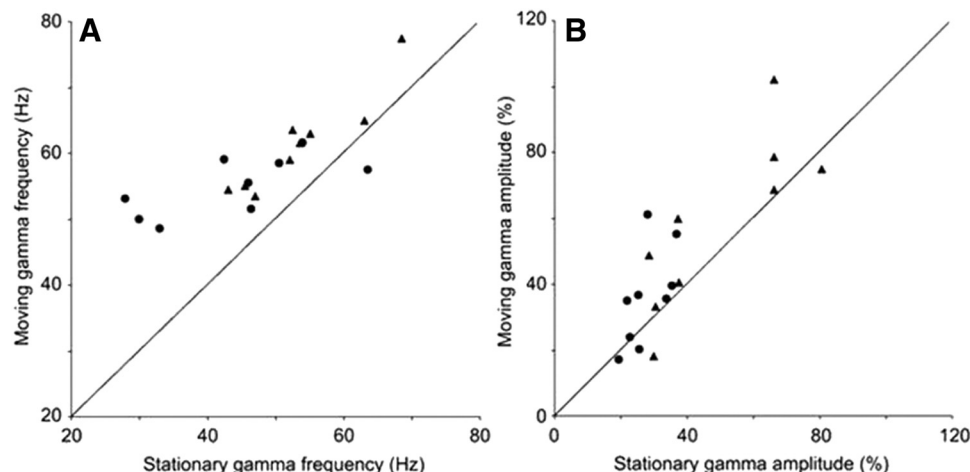

FIG. 5. In *A*, the gamma oscillation frequency for moving stimuli is plotted against the oscillation frequency for stationary stimuli from *experiment 2*. Each point is data from 1 observer. Triangles represent the initial gamma onset "spike" response, circles represent the sustained gamma response that occurs for the entire stimulus presentation time. All but one datum lie above the $y = x$ line, indicating that for both responses, the gamma oscillation frequency for moving stimuli is higher than for stationary. In *B*, a similar plot is shown for response amplitude, this shows a trend toward higher amplitude responses for moving stimuli.
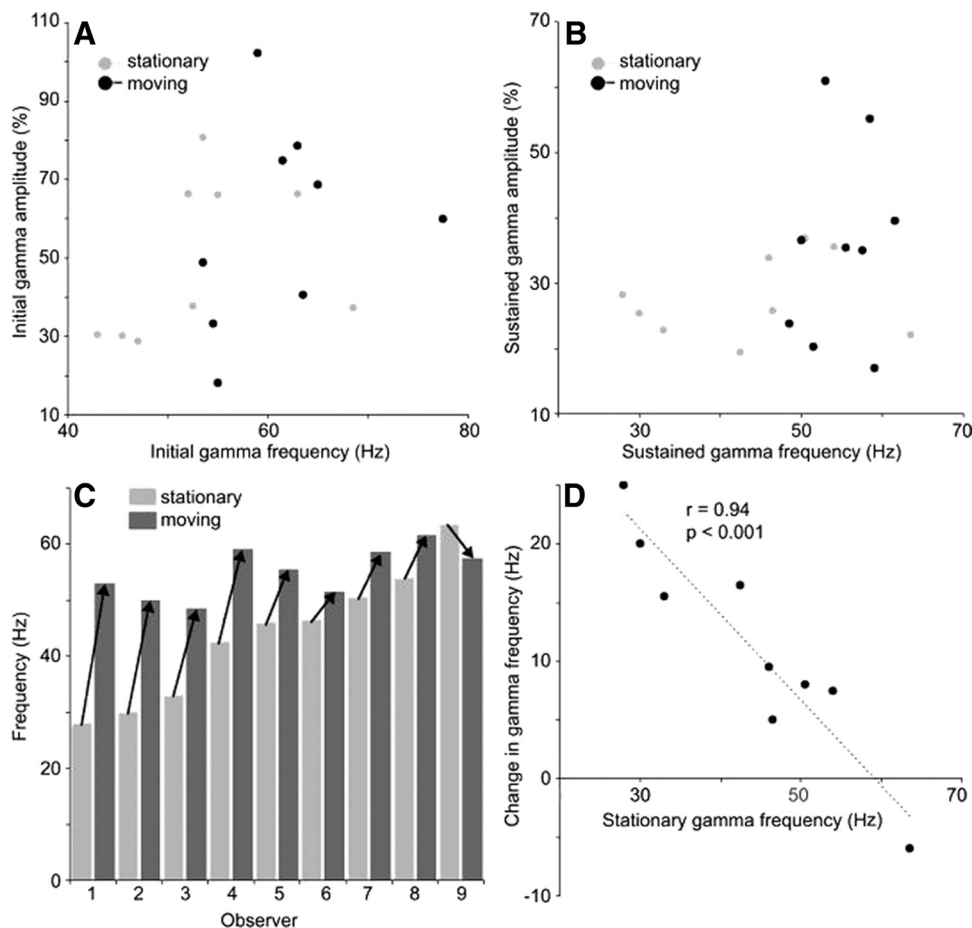
FIG. 6. In *A* and *B,* the relationship between gamma amplitude and gamma frequency is investigated for *experiment 2.* Each data point represents the response of 1 observer to a single condition: light gray dots represent stationary stimuli; black dots represent moving stimuli. In *A,* the amplitude/frequency relationship is plotted for the initial gamma onset spike, and in *B,* the same analysis is performed for the sustained gamma response. No robust trend was observed in any of the conditions, i.e., there was no apparent relationship between gamma response amplitude and frequency. In *C,* the frequency of the sustained gamma response is plotted for each observer. The responses are sorted so that *observer 1* has the lowest stationary gamma frequency and *observer 9* the highest. It is clear that there is a large range in the peak frequency of the response, ranging from 28 to 64 Hz. The black arrows depict the change in gamma frequency between stationary and moving stimuli for each observer and show that the largest frequency shifts are present in those observers with the lowest gamma frequency for stationary stimuli. This is more explicit in *D* where the magnitude of gamma frequency increase, between stationary and moving stimuli, is plotted as a function of the sustained gamma response frequency for stationary stimuli. There is a highly significant linear correlation between these 2 parameters, suggesting, perhaps, a saturation effect that limits the maximum frequency of response for all observers.

long presentation was the "gold standard." SAM analyses were performed using a range of simulated presentation times (0.2–1.9 s), and the magnitude of the mean gamma response and the spatial location were compared with the original values (2 s time windows). The reconstructed gamma amplitude increased rapidly as stimulus duration increased from 0.2 to 0.5 s and then continued to increase more gradually. In comparison, the spatial localization error dropped rapidly as duration increased from 0.2 to 0.8 s. A stimulus duration of 0.8 s would recover 87% of the signal and result in a relative localization error of 1.7 mm, which is less than half the SAM voxel size.

DISCUSSION

In this paper, we have demonstrated how the presentation of simple visual grating stimuli evoke and induce a rich set of oscillatory responses in early visual cortex, including evoked onset responses, sustained alpha/beta power reductions, a rapidly adapting gamma onset spike and a sustained gamma power increase from around 25 to 90 Hz. These results are in general agreement with previous MEG studies using similar stationary gratings (Adjamian et al. 2004; Hadjipapas et al. 2007; Hall et al. 2005) and contracting, circularly sinusoidal gratings (Hoogenboom et al. 2006). An analysis of the magnitude of the different response components across individuals suggests that they are independent measures, for example, the magnitude of the induced gamma response is not correlated with the magnitude of any of the other components, such as the evoked response or alpha/beta power reductions. Using the current experimental

design, these effects were only measurable for grating presentations close to the fovea and not for eccentric presentations. This may be partially explained by the spatial-frequency used, 3 cpd, being nonoptimal for detection in the periphery. It should also be noted that, unlike previous MEG studies using temporally reversing stimuli (Fawcett et al. 2004; Muthukumaraswamy and Singh 2008), we did not observe a driven, steady-state, evoked response at a harmonic of the stimulus frequency. This is consistent with previous EEG studies in which the absence of a steady-state response to drifting gratings has been previously reported (Burr et al. 1987) and may reflect spatial pooling of responses at different phases.

The results presented here show an excellent correspondence with previous invasive recordings in both cat and monkey. In LFP recordings in cat (Kayser et al. 2003; Kruse and Eckhorn 1996; Siegel and König 2003), the same richness of response components has been observed in response to simple grating stimuli, namely an evoked onset response, an onset gamma spike and sustained induced gamma responses. In one of these studies, stimulus-induced power reductions in the alpha/beta band (<20 Hz) were also observed at the same time and location as 30 to 60 Hz narrow band gamma power increases (Kayser et al. 2003). This same study also showed that gamma oscillations appeared in V1 around 150 ms after stimulus onset, a similar latency to that reported here (Fig. 3*G*). In awake macaque, Henrie and Shapley (2005) showed that simple grating stimuli induced sustained gamma oscillations across a wide frequency range $\leq$200 Hz with the strongest changes in

the 25 to 90 Hz range, consistent with the results of the current study. Similarly, in another study of awake macaque, the strongest V1 gamma oscillations in response to square- and sine-wave gratings were found in the 20 to 70 Hz frequency range and, as with the current study, were sustained for the entire 2 to 2.5 s presentation time (Friedman-Hill et al. 2000). Also in macaque, electrocorticography (EcoG) was used to record evoked and induced gamma responses from the surface of V1 that were remarkably similar in their morphology to the results described in the current study (Rols et al. 2001, their Figs. 1 and 2). These studies indicate that despite the much larger spatial scales, MEG/SAM may provide a powerful window into the neurophysiological properties of visual cortex in humans.

The main finding of this study is that in early medial visual cortex, the induced gamma frequency response is the only component that is sensitive to the presence of visual motion in the stimulus. As with previous animal recordings within V1 (see preceding text), there was no evidence of a reduction in the amplitude of this sustained gamma oscillation, and this is consistent with several neuroimaging studies indicating that motion adaptation occurs in multiple higher visual motion processing areas (reviewed in Mather et al. 2008). Together with previous MEG studies (Adjamian et al. 2004; Hall et al. 2005), this shows that the spectral properties of gamma oscillations in early visual cortex are dependent on stimulus properties such as spatial frequency, contrast, and movement. This stimulus dependence may be due to optimally driving single units connected in a recurrent network (Henrie and Shapley 2005) and may have a possible role in perceptual binding or feature integration (Singer and Gray 1995). In contrast, the evoked response in the virtual electrodes did not show any difference between the stationary and moving conditions. The latencies were ∼85 ms, which is earlier than would be expected for a motion-related potential (see Heinrich 2007) and are similar to those of the early C1 component of the pattern onset potential (Im et al. 2007). Similarly, the alpha/beta power reductions did not show any difference between conditions. In *experiment 1,* where button presses were only required at the end of the stationary-moving combined trial, alpha/beta power reductions do appear to be stronger for moving stimuli compared with stationary. However, this finding was not replicated in *experiment 2,* where stationary and moving trials were separate and presented randomly. This suggests that the alpha/beta desynchronization seen in both experiments is not stimulus-driven but is more related to the observer's attentional state as they prepare to make a button response at the trial offset.

The gamma oscillations in human early visual cortex occurred at a higher frequency for moving than stationary stimuli. Again, there is strong evidence for this in both cat and macaque experiments. Gray et al. (1990) showed that gamma frequency increased monotonically with stimulus velocity, although responses to stationary stimuli in the anesthetized cat were much weaker or absent. In a study of awake macaques (Friedman-Hill et al. 2000), stationary and moving gratings elicited LFP gamma oscillations of comparable amplitudes as we report here. Importantly, they also found that stationary stimuli induced LFP gamma at a lower frequency (36 ± 6 Hz) than moving stimuli (47 ± 8 Hz). This represents a mean frequency difference of around 11 Hz, which is remarkably similar to the current MEG study: In *experiment 1,* we found a mean differ-

ence of 7.5 Hz (stationary: 44 ± 1 Hz; moving: 51 ± 2 Hz) and in *experiment 2* a mean difference of 11 Hz (stationary: 44 ± 4 Hz; moving = 55 ± 1 Hz) for the sustained gamma response. This variation in spectral properties for moving versus stationary stimuli demonstrates the importance of not averaging over too wide a spectral window when analyzing these responses. For example, in Fig. 3*G,* activity within primary visual cortex is averaged between 25 and 85 Hz, and no difference is seen between stationary and moving stimuli. Differential effects are only seen when narrower windows are used, such as 55–65 Hz.

The association of higher gamma frequencies with moving compared with stationary stimuli may reflect a functional role of these frequencies in encoding the presence of visual motion or flicker. In a recent human MEG study, Siegel et al. (2007) showed that increasing motion coherence was correlated with increases in 60 to 100 Hz activity in extra-striate visual areas, while at lower gamma frequencies the activity was similar for all motion coherencies. Siegel et al. (2007) did not use a static stimulus condition, so we cannot directly compare their results with our findings, but it does demonstrate that higher gamma frequencies may carry more motion-specific information than lower frequencies. It should be noted that drifting stimuli also have an associated temporal frequency (flicker), and early visual cortex may be more sensitive to changes in temporal frequency than velocity per se (Foster et al. 1985). Alternatively, the shift to higher frequencies may reflect stronger or more salient stimuli rather than motion or temporal frequency. A shift to increased frequencies with increasing mean activation strength has been predicted by a recent modeling study (Kilner et al. 2005), and fMRI studies have shown that moving stimuli generate a larger BOLD response in V1 compared with static stimuli (Singh et al. 2000; Tootell et al. 1995). However, not enough is known about the coupling mechanism between the electrophysiological responses recorded with MEG and the BOLD response to be clear what effect spectral changes, such as the oscillation frequency increase we observe here, would have on the BOLD response. In addition, as shown in Fig. 4, we found no evidence of a shift in the entire spectrum. In particular, low frequencies (alpha/beta) were unchanged by the presence of motion. Also to our knowledge, no animal or human EEG/MEG study has reported such large changes in oscillation frequency with changes in other stimulus parameters. In humans, Hall et al. (2005) reported increases in primary visual cortex gamma amplitude with increases in stimuli contrast, but they did not report a frequency increase. However, this may be due to their use of a relatively wide, 30–70 Hz, analysis band that, as we discuss in the preceding text, may wash out stimulus-related spectral changes. In another human MEG study, Hadjipapas et al. (2007) showed that varying the spatial frequency of a static grating patch changed the spectral properties of the induced response, but these were very subtle changes in spectral shape compared with the large differences in narrow-band oscillation frequency that we report here. It is also possible that in the current study, participants attended more to the moving stimulus than the stationary. Although the task was to simply press a button when the stimulus patch disappeared and was the same for both stationary and drifting stimuli, we cannot rule out a general increased level of attention or arousal to the moving stimuli.

There was an increase in gamma amplitude for moving compared with static stimuli in *experiment 1* ($P < 0.05$) and a

trend toward an increase in *experiment 2* ($P < 0.1$). Some animal studies have demonstrated stronger gamma oscillations to moving than stationary stimuli (Gray et al. 1990; Kruse and Eckhorn 1996), although others have shown no difference (Friedman-Hill et al. 2000). As discussed in the preceding text, it is possible that moving stimuli were associated with higher levels of attention. Consistent with this, previous studies have shown increased gamma oscillation amplitude with increased levels of selective attention in monkey (Fries et al. 2001) and human (Gruber et al. 1999). Attention related gamma oscillations may reflect an increase in inter-regional coherence as it has previously been shown that attention modulates coherence but not firing rate in monkey V4 (Fries et al. 2001), and they may have a function in optimal gain control of spiking rate, thereby enhancing the detection and discriminability of stimuli (Börgers et al. 2005; Masuda and Doiron 2007; Schaefer et al. 2006; Tiesinga et al. 2004).

In the current study, there is a large between-observer variation, from 28 to 64 Hz, in the peak frequency of sustained gamma oscillations induced by the presentation of static gratings. A similar variation in the oscillation frequency has been observed in macaque monkey with peak frequencies varying between 30 and 60 Hz (Friedman-Hill et al. 2000; Rols et al. 2001). The results of a modeling study suggest that oscillation frequency may depend on the excitation/inhibition balance within local re-entrant circuits with GABA-mediated inhibition processes dominant in the relatively low-frequency gamma domain (Brunel and Wang 2003). This study associated increased inhibition via GABA with increased oscillation frequency, and consequently individual differences in frequency may reflect how local networks are constructed or normal variability in the levels of neurotransmitters such as GABA (or a combination of both). A shift in the excitation/inhibition balance could also explain stimulus-driven changes in gamma oscillation frequency as found in the current study. If gamma frequency can be used as a window to GABA-mediated inhibition, then the kind of experiment we describe here may be useful within the context of studying pharmacological manipulations, e.g., morphine (Whittington et al. 1998), or specific diseases, e.g., epilepsy (Parra et al. 2003) and schizophrenia (Gonzalez-Burgos and Lewis 2008), known to compromise excitatory/inhibitory neurotransmitters such as GABA.

Interestingly, the higher the oscillation frequency for static stimuli, the smaller the frequency increase for moving stimuli. One speculative interpretation of this is that there is an upper oscillation frequency for stimulus driven gamma responses, and some individuals are naturally close to this limit. This is partially supported by monkey studies, in that stimulus-specific effects fall off quickly > 70 Hz (Friedman-Hill et al. 2000; Henrie and Shapley 2005). It has also been reported that even for high stimulus velocities, stimulus driven oscillations in macaque do not exceed 70 Hz (Maldonado and Gray 1997), which is similar to the saturation limit we observe in the current study. Human implanted electrode studies in patients suggest an accelerated falloff in the intrinsic spectrum >70 Hz, which is fundamentally related to the time constants of oscillatory neuronal circuits (Miller et al. 2007). So the magnitude of any higher frequency gamma oscillations in human V1 may be too small to be measured using either MEG or EEG, perhaps due to higher frequency oscillations being generated by more focal networks containing less neurons (Pfurtscheller and Lopes da Silva 1999).

In this study, areas of increased gamma activity are localized to the left early visual cortex, consistent with viewing a right visual field stimulus and the retinotopic nature of early visual cortex. Although previous animal studies have demonstrated that motion-induced gamma frequency increases occur in V1 (Friedmann-Hill et al. 2000), we cannot claim that the similar phenomenology we have measured in humans using MEG is also restricted to V1. For example, in some cases, the areas of increased gamma power, as determined with SAM, were spread over a relatively large area of visual cortex and may have included more than one visual area (Fig. 1A).

In contrast to medial visual cortex, no evidence was found of activation of lateral motion-sensitive areas, such as V3A or V5/MT, by the drifting grating stimulus. This may seem strange, as the drifting grating was perceived as moving by the observers. However, the drifting grating was a nonoptimal stimulus for both V3A and V5/MT in terms of spatial frequency, velocity, and direction. These motion-sensitive areas are strongly low-pass tuned for spatial frequency as has been previously demonstrated in humans using both fMRI (Henriksson et al. 2008; Singh et al. 2000) and MEG (Anderson et al. 1996). Singh et al. (2000) reported that BOLD activations, in both V3A and V5, to gratings with spatial frequencies of 1 and 4 cpd were only 40–50% the magnitude of those to 0.5 cpd gratings. In addition, their presentation time (27 s) was substantially longer than ours, and this may have allowed responses to summate and become measurable.

In comparison, using MEG, Anderson et al. (1996) found that evoked responses in V5 were barely measurable when spatial frequency reached 4 cpd. Kawakami et al. (2002) investigated the effect of a wide range of velocities (0.4– 500°/s) on activations in V5/MT and found differences between fMRI and MEG responses. While fMRI revealed activations to fast and slow motion, the MEG responses were highly tuned, with faster speeds eliciting larger responses— velocities similar to ours ($<2°/s$) were very poor at eliciting responses. Concern over magnetic field cancellation in primary visual cortex, due to its cruciform structure and retinotopic nature, was the reason the stimulus was presented in one visual quadrant, thereby only activating one quadrant of primary visual cortex. However, this may also have reduced activation in higher visual areas, which are known to have much larger receptive fields. Indeed Henriksson et al. (2008) demonstrated not only larger activations in V3A and V5 when stimuli were presented centrally versus in a quadrant, but also steeper spatial frequency tuning curves when presented in a quadrant. Finally, the direction of motion may influence the magnitude of responses in V5/MT as it has been shown that evoked responses measured with MEG were larger to expanding motion than to rotational or translational (as used here) (Holliday and Meese 2005). Thus for a number of reasons, the drifting grating used in this study was a poor stimulus for both V3A and V5/MT.

One possible explanation for moving stimuli inducing higher gamma frequencies is that there may be differences in the levels of eye movements between the moving and stationary conditions. Such movements could be either voluntary eye movements or involuntary fixation movements, such as microsaccades. First considering voluntary saccades, it has been shown that these induce changes in the magnitude of the

BOLD response in human V1 (Bodis-Wallner et al. 1997; Rieger et al. 2008; Sylvester et al. 2005). We did not record eye movements so cannot definitively address this issue. However, if participants were making larger and more frequent eye movements during either stimulus condition, compared with baseline, then we would have expected to see SAM activity localized to the eye area due to eye muscle activity, temporal transients in the time-frequency plots reflecting rapid movements of the stimulus across the retina (e.g., Kayser et al. 2003), or bilateral activation of visual cortex due to the stimulus being foveated. No evidence was found for any of these, with SAM gamma activity observed only in the expected contralateral hemisphere, suggesting that participants were, in general, correctly fixating the stimulus. However, the issue of involuntary fixation saccades remains. Observers are unaware of making these small, rapid eye movements, which may play a functional role in preventing perceptual fading of stimuli (see Engbert 2006 for a review). It has been recently suggested that induced gamma oscillations recorded from the scalp using EEG may directly reflect eye-muscle artifacts from microsaccades (or neck/shoulder muscle artifacts) (Whitham et al. 2008) rather than neural activity (Yuval-Greenberg et al. 2008; and see comment Fries et al. 2008). However, as pointed out by the authors (Fries et al. 2008; Yuval-Greenberg et al. 2008), there is good reason to believe that such artifacts will not contaminate MEG studies of gamma oscillations. Furthermore, the morphology of the spectral response reported here differs from that recorded with EEG (Yuval-Greenberg et al. 2008) but has a striking similarity to that recorded intracranially in animal studies (e.g., Rols et al. 2001), suggesting that MEG-measured induced gamma reflects neural, rather than muscle, activity. However, there is evidence that neural activity in visual areas may be directly modulated by small fixation eye movements. A recent study demonstrated that switches in stimulus visibility correlated both with modulations in microsaccade rate and modulations of human V1 BOLD responses in an fMRI experiment (Hsieh and Tse 2009), and animal studies have shown microsaccades to have direct effects on neuronal firing in V1 (Kagan et al. 2008; Leopold and Logothetis 1998; Martinez-Conde et al. 2000; Snodderly et al. 2001). Thus differences in gamma responses when viewing moving versus stationary stimuli, and inter-participant variability, could still reflect differences in the magnitude and frequency of small fixation eye movements. Future studies could investigate this by the off-line recording of microsaccades in each individual using eye trackers with higher spatial and temporal resolution than those commonly available in MEG and fMRI labs.

In terms of other artifacts, there was no evidence of activation in the eyes that would have been expected with SAM analysis if eye blinks were contaminating the data (Bardouille et al. 2006). This is important as eye blinks have also been associated with an increase in gamma activity in occipital cortex ~200–400 ms after blinking (Bardouille et al. 2006). However, even if eye-blink-related occipital contamination had occurred, then the transient effects reported by Bardouille et al. are not sufficient to explain the results reported here.

Finally, future studies could further examine the dependency of gamma frequencies on parameters such as velocity, temporal frequency and spatial frequency. For example, in a study of cat V1 (Kayser et al. 2003) it was shown that the broad range of spatial frequencies present in natural images generate a sustained gamma response across a broad range of frequencies, even if the scene translates smoothly at a single velocity. Similarly, a recent human MEG study (Hadjipapas et al. 2007) showed the shape of the gamma power spectrum to be subtly related to the spatial frequency content of the stimulus. These results suggest that the shape and width of the gamma spectrum is determined by the spatial frequency content of the stimulus, while our current study suggests that the center frequency of the response is determined by either the velocity or temporal frequency of the stimulus. By repeating the current study with a variety of spatial and temporal frequencies, the precise relationship between these stimulus parameters and the resulting gamma spectrum could be elucidated. Such a study could also investigate whether temporal frequency or velocity is the determinant of gamma frequency in medial cortex and hence provide a direct comparison with the finding in cat that frequency increases monotonically with velocity (Gray et al. 1990). Such experiments can be made more efficient by using shorter trials (than the 2.0 to 2.4 s presentation duration used in the current study) as our simulations demonstrate that trials of only 0.8 s can be sufficient to accurately localize and characterize visual gamma responses.

In summary, we have shown a rich mixture of evoked and induced responses from human early visual cortex with as few as 50 trials per condition. Of particular interest is the nonphase locked increase in gamma activity (25–90 Hz) that was sustained during stimulus presentation. The frequency of this power increase was higher for moving than stationary stimuli, suggesting that early visual areas encode moving and stationary percepts via activity at higher and lower gamma frequencies, respectively.

REFERENCES

Adjamian P, Holliday I, Barnes G, Hillebrand A, Hadjipapas A, Singh K. Induced visual illusions and gamma oscillations in human primary visual cortex. *Eur J Neurosci* 20: 587–592, 2004.

Anderson S, Holliday I, Singh K, Harding G. Localization and functional analysis of human cortical area V5 using magneto-encephalography. *Proc Biol Sci* 263: 423–431, 1996.

Bardouille T, Picton TW, Ross B. Correlates of eye blinking by synthetic aperture magnetometry. *Clin Neurophysiol* 117: 952–958, 2006.

Behrendt RP, Young C. Hallucinations in schizophrenia, sensory impairment, and brain disease: a unifying model. *Behav Brain Sci* 27: 771–+, 2004.

Belitski A, Gretton A, Magri C, Murayama Y, Montemurro M, Logothetis N, Panzeri S. Low-frequency local field potentials and spikes in primary visual cortex convey independent visual information. *J Neurosci* 28: 5696–5709, 2008.

Bodis-Wollner I, Bucher SF, Seelos KC, Paulus W, Reiser M, Oertel WH. Functional MRI mapping of occipital and frontal cortical activity during voluntary and imagined saccades. *Neurol* 49: 416–420, 1997.

Brookes M, Vrba J, Robinson S, Stevenson C, Peters A, Barnes G, Hillebrand A, Morris P. Optimising experimental design for MEG beamformer imaging. *Neuroimage* 39: 1788–1802, 2008.

Brunel N, Wang X. What determines the frequency of fast network oscillations with irregular neural discharges? I. Synaptic dynamics and excitation-inhibition balance. *J Neurophysiol* 90: 415–430, 2003.

Burr D, Fiorentini A, Morrone M. Electrophysiological correlates of positive and negative afterimages. *Vision Res* 27: 201–207, 1987.

Börgers C, Epstein S, Kopell N. Background gamma rhythmicity and attention in cortical local circuits: a computational study. *Proc Natl Acad Sci USA* 102: 7002–7007, 2005.

Campbell F, Robson J. Application of Fourier analysis to the visibility of gratings. *J Physiol* 197: 551–566, 1968.

Cheyne D, Gaetz W, Garnero L, Lachaux J, Ducorps A, Schwartz D, Varela F. Neuromagnetic imaging of cortical oscillations accompanying tactile stimulation. *Brain Res Cogn Brain Res* 17: 599–611, 2003.

Eckhorn R, Bauer R, Jordan W, Brosch M, Kruse W, Munk M, Reitboeck H. Coherent oscillations: a mechanism of feature linking in the visual cortex? Multiple electrode and correlation analyses in the cat. *Biol Cybern* 60: 121–130, 1988.

Engbert R. Microsaccades: a microcosm for research on oculomotor control, attention, and visual perception. In: *Progress in Brain Research: Visual Perception. Fundamentals of Vision: Low and Mid-Level Processes in Perception*, edited by Martinez-Conde S, Macknik SL, Martinez LM, Alonso JM, Tse PU. Amsterdam: Elsevier, 2006, vol. 154, part 1, p. 177–192.

Engel AK, Fries P, Singer W. Dynamic predictions: oscillations and synchrony in top-down processing. *Nat Rev Neurosci* 2: 704–716, 2001.

Engel AK, Konig P, Kreiter AK, Schillen TB, Singer W. Temporal coding in the visual cortex—new vistas on integration in the nervous system. *Trends Neurosci* 15: 218–226, 1992.

Fawcett I, Barnes G, Hillebrand A, Singh K. The temporal frequency tuning of human visual cortex investigated using synthetic aperture magnetometry. *Neuroimage* 21: 1542–1553, 2004.

Foster K, Gaska J, Nagler M, Pollen D. Spatial and temporal frequency selectivity of neurons in visual cortical areas V1 and V2 of the macaque monkey. *J Physiol* 365: 331–363, 1985.

Friedman-Hill S, Maldonado P, Gray C. Dynamics of striate cortical activity in the alert macaque. I. Incidence and stimulus-dependence of gamma-band neuronal oscillations. *Cereb Cortex* 10: 1105–1116, 2000.

Frien A, Eckhorn R, Bauer R, Woelbern T, Gabriel A. Fast oscillations display sharper orientation tuning than slower components of the same recordings in striate cortex of the awake monkey. *Eur J Neurosci* 12: 1453–1465, 2000.

Fries P, Nikolic D, Singer W. The gamma cycle. *Trends Neurosci* 30: 309–316, 2007.

Fries P, Reynolds J, Rorie A, Desimone R. Modulation of oscillatory neuronal synchronization by selective visual attention. *Science* 291: 1560–1563, 2001.

Fries P, Scheeringa R, Oostenveld R. Finding gamma. *Neuron* 58: 303–305, 2008.

Gail A, Brinksmeyer H, Eckhorn R. Perception-related modulations of local field potential power and coherence in primary visual cortex of awake monkey during binocular rivalry. *Cereb Cortex* 14: 300–313, 2004.

Gonzalez-Burgos G, Lewis D. GABA neurons and the mechanisms of network oscillations: implications for understanding cortical dysfunction in schizophrenia. *Schizophr Bull* 34: 944–961, 2008.

Gray C, Engel A, König P, Singer W. Stimulus-dependent neuronal oscillations in cat visual cortex: receptive field properties and feature dependence. *Eur J Neurosci* 2: 607–619, 1990.

Gray C, König P, Engel A, Singer W. Oscillatory responses in cat visual cortex exhibit inter-columnar synchronization which reflects global stimulus properties. *Nature* 338: 334–337, 1989.

Gruber T, Müller M, Keil A, Elbert T. Selective visual-spatial attention alters induced gamma band responses in the human EEG. *Clin Neurophysiol* 110: 2074–2085, 1999.

Gur M, Beylin A, Snodderly DM. Response variability of neurons in primary visual cortex (V1) of alert monkeys. *J Neurosci* 17: 2914–2920, 1997.

Hadjipapas A, Adjamian P, Swettenham J, Holliday I, Barnes G. Stimuli of varying spatial scale induce gamma activity with distinct temporal characteristics in human visual cortex. *Neuroimage* 35: 518–530, 2007.

Hall S, Holliday I, Hillebrand A, Singh K, Furlong P, Hadjipapas A, Barnes G. The missing link: analogous human and primate cortical gamma oscillations. *Neuroimage* 26: 13–17, 2005.

Heinrich SP. A primer on motion visual evoked potentials. *Doc Ophthalmol* 114: 83–105, 2007.

Henriksson L, Nurminen L, Hyvarinen A, Vanni S. Spatial frequency tuning in human retinotopic visual areas. *J Vision* 8: 1–13, 2008.

Henrie J, Shapley R. LFP power spectra in V1 cortex: the graded effect of stimulus contrast. *J Neurophysiol* 94: 479–490, 2005.

Hillebrand A, Barnes G. Beamformer analysis of MEG data. *Int Rev Neurobiol* 68: 149–171, 2005.

Hillebrand A, Singh K, Holliday I, Furlong P, Barnes G. A new approach to neuroimaging with magnetoencephalography. *Hum Brain Mapp* 25: 199–211, 2005.

Hinds OP, Rajendran N, Polimeni JR, Augustinack JC, Wiggins G, Wald LL, Rosas HD, Potthast A, Schwartz EL, Fischl B. Accurate prediction of V1 location from cortical folds in a surface coordinate system. *Neuroimage* 39: 1585–1599, 2008.

Holliday IE, Meese TS. Neuromagnetic evoked responses to complex motions are greatest for expansion. *Int J Psychophys* 55: 145–157, 2005.

Hoogenboom N, Schoffelen J, Oostenveld R, Parkes L, Fries P. Localizing human visual gamma-band activity in frequency, time and space. *Neuroimage* 29: 764–773, 2006.

Hsieh P-J, Tse PU. Microsaccade rate varies with subjective visibility during motion-induced blindness. *PLoS One* 4: e5163, 2009.

Huang M, Mosher J, Leahy R. A sensor-weighted overlapping-sphere head model and exhaustive head model comparison for MEG. *Phys Med Biol* 44: 423–440, 1999.

Im C, Gururajan A, Zhang N, Chen W, He B. Spatial resolution of EEG cortical source imaging revealed by localization of retinotopic organization in human primary visual cortex. *J Neurosci Methods* 161: 142–154, 2007.

Jensen O, Kaiser J, Lachaux J. Human gamma-frequency oscillations associated with attention and memory. *Trends Neurosci* 30: 317–324, 2007.

Kagan I, Gur M, Snodderly DM. Saccades and drifts differentially modulate neuronal activity in V1: effects of retinal image motion, position, and extraretinal influences. *J Vis* 8: 14–19, 2008.

Kawakami O, Kaneoke Y, Maruyama K, Kakigi R, Okada T, Sadato N, Yonekura Y. Visual detection of motion speed in humans: spatiotemporal analysis by fMRI and MEG. *Hum Brain Mapp* 16: 104–118, 2002.

Kayser C, Salazar R, Konig P. Responses to natural scenes in cat V1. *J Neurophysiol* 90: 1910–1920, 2003.

Kilner J, Mattout J, Henson R, Friston K. Hemodynamic correlates of EEG: a heuristic. *Neuroimage* 28: 280–286, 2005.

Krishnan GP, Skosnik PD, Vohs JL, Busey TA, O'Donnell BF. Relationship between steady-state and induced gamma activity to motion. *Neuroreport* 16: 625–630, 2005.

Kruse W, Eckhorn R. Inhibition of sustained gamma oscillations (35–80 Hz) by fast transient responses in cat visual cortex. *Proc Natl Acad Sci USA* 93: 6112–6117, 1996.

Leopold DA, Logothetis NK. Microsaccades differentially modulate neural activity in the striate and extrastriate visual cortex. *Exp Brain Res* 123: 341–345, 1998.

Logothetis N, Pauls J, Augath M, Trinath T, Oeltermann A. Neurophysiological investigation of the basis of the fMRI signal. *Nature* 412: 150–157, 2001.

Maldonado P, Friedman-Hill S, Gray C. Dynamics of striate cortical activity in the alert macaque. II. Fast time scale synchronization. *Cereb Cortex* 10: 1117–1131, 2000.

Maldonado P, Gray C. Frequency of neuronal oscillations in monkey striate cortex is modulated by stimulus velocity. *Soc Neurosci Abstr* 23: 13, 1997.

Martinez-Conde S, Macknik SL, Hubel DH. Microsaccadic eye movements and firing of single cells in the striate cortex of macaque monkeys. *Nat Neurosci* 3: 251–258, 2000.

Masuda N, Doiron B. Gamma oscillations of spiking neural populations enhance signal discrimination. *PLoS Comput Biol* 3: e236, 2007.

Mather G, Pavan A, Campana G, Casco C. The motion aftereffect reloaded. *Trends Cogn Sci* 12: 481–487, 2008.

Melloni L, Molina C, Pena M, Torres D, Singer W, Rodriguez E. Synchronization of neural activity across cortical areas correlates with conscious perception. *J Neurosci* 27: 2858–2865, 2007.

Miller K, Sorensen L, Ojemann J, Nijs M. ECoG observations of power-law scaling in the human cortex. arXiv:0712.0846v1 [q-bio.NC], 2007.

Muthukumaraswamy S, Singh K. Spatiotemporal frequency tuning of BOLD and gamma band MEG responses compared in primary visual cortex. *Neuroimage* 40: 1552–1560, 2008.

Nichols T, Holmes A. Nonparametric permutation tests for functional neuroimaging: a primer with examples. *Hum Brain Mapp* 15: 1–25, 2002.

Palva S, Palva JM. New vistas for alpha-frequency band oscillations. *Trends Neurosci* 30: 150–158, 2007.

Pareti G, De Palma A. Does the brain oscillate? The dispute on neuronal synchronization. *Neurol Sci* 25: 41–47, 2004.

Parra J, Kalitzin S, Iriarte J, Blanes W, Velis D, Lopes da Silva F. Gamma-band phase clustering and photosensitivity: is there an underlying mechanism common to photosensitive epilepsy and visual perception? *Brain* 126: 1164–1172, 2003.

Parra J, Kalitzin SN, Lopes da Silva FHL. Photosensitivity and visually induced seizures. *Curr Opin Neurol* 18: 155–159, 2005.

Pfurtscheller G, Lopes da Silva F. Event-related EEG/MEG synchronization and desynchronization: basic principles. *Clin Neurophysiol* 110: 1842–1857, 1999.

Rieger JW, Schoenfeld MA, Heinze H-J, Bodis-Wollner I. Different spatial organizations of saccade related BOLD-activation in parietal and striate cortex. *Brain Res* 1233: 89–97, 2008.

Robinson S, Vrba J. Functional neuroimaging by synthetic aperture magnetometry (SAM). In: *Recent Advances in Biomagnetism,* edited by Yoshimoto T, Kotani M, Kuriki S, Karibe H, Nakasato N. Sendai, Japan: Tohoku University Press, 1999, p. 302–305.

Rols G, Tallon-Baudry C, Girard P, Bertrand O, Bullier J. Cortical mapping of gamma oscillations in areas V1 and V4 of the macaque monkey. *Vis Neurosci* 18: 527–540, 2001.

Schaefer A, Angelo K, Spors H, Margrie T. Neuronal oscillations enhance stimulus discrimination by ensuring action potential precision. *PLoS Biol* 4: e163, 2006.

Shapley R, Hawken M, Ringach D. Dynamics of orientation selectivity in the primary visual cortex and the importance of cortical inhibition. *Neuron* 38: 689–699, 2003.

Siegel M, Donner T, Oostenveld R, Fries P, Engel A. High-frequency activity in human visual cortex is modulated by visual motion strength. *Cereb Cortex* 17: 732–741, 2007.

Siegel M, König P. A functional gamma-band defined by stimulus-dependent synchronization in area 18 of awake behaving cats. *J Neurosci* 23: 4251–4260, 2003.

Singer W, Gray C. Visual feature integration and the temporal correlation hypothesis. *Annu Rev Neurosci* 18: 555–586, 1995.

Singh K, Barnes G, Hillebrand A. Group imaging of task-related changes in cortical synchronisation using nonparametric permutation testing. *Neuroimage* 19: 1589–1601, 2003.

Singh K, Smith A, Greenlee M. Spatiotemporal frequency and direction sensitivities of human visual areas measured using fMRI. *Neuroimage* 12: 550–564, 2000.

Snodderly DM, Kagan I, Gur M. Selective activation of visual cortex neurons by fixational eye movements: Implications for neural coding. *Vis Neurosci* 18: 259–277, 2001.

Super H, van der Togt C, Spekreijse H, Lamme VAF. Correspondence of presaccadic activity in the monkey primary visual cortex with saccadic eye movements. *Proc Natl Acad Sci USA* 101: 3230–3235, 2004.

Sylvester R, Haynes J-D, Rees G. Saccades differentially modulate human LGN and V1 responses in the presence and absence of visual stimulation. *Curr Biol* 15: 37–41, 2005.

Tallon-Baudry C, Bertrand O. Oscillatory gamma activity in humans and its role in object representation. *Trends Cogn Sci* 3: 151–162, 1999.

Tiesinga P, Fellous J, Salinas E, José J, Sejnowski T. Inhibitory synchrony as a mechanism for attentional gain modulation. *J Physiol* 98: 296–314, 2004.

Tootell R, Reppas J, Kwong K, Malach R, Born R, Brady T, Rosen B, Belliveau J. Functional analysis of human MT and related visual cortical areas using magnetic resonance imaging. *J Neurosci* 15: 3215–3230, 1995.

Vrba J, Robinson S. Signal processing in magnetoencephalography. *Methods* 25: 249–271, 2001.

Walters NB, Egan GF, Kril JJ, Kean M, Waley P, Jenkinson M, Watson JDG. In vivo identification of human cortical areas using high resolution MRI: an approach to cerebral structure-function correlation. *Proc Natl Acad Sci USA* 100: 2981–2986, 2003.

Whitham EM, Lewis T, Pope KJ, Fitzgibbon SP, Clark CR, Loveless S, DeLosAngeles D, Wallace AK, Broberg M, Willoughby JO. Thinking activates EMG in scalp electrical recordings. *Clin Neurophysiol* 119: 1166–1175, 2008.

Whittington M, Traub R, Faulkner H, Jefferys J, Chettiar K. Morphine disrupts long-range synchrony of gamma oscillations in hippocampal slices. *Proc Natl Acad Sci USA* 95: 5807–5811, 1998.

Womelsdorf T, Fries P. Neuronal coherence during selective attentional processing and sensory-motor integration. *J Physiol* 100: 182–193, 2006.

Yuval-Greenberg S, Tomer O, Keren AS, Nelken I, Deouell LY. Transient induced gamma-band response in EEG as a manifestation of miniature saccades. *Neuron* 58: 429–441, 2008.